

Gas Permeability and Free Volume of Highly Branched Substituted Acetylene Polymers

Yu. P. Yampolskii,^{*,†} A. P. Korikov,[†] V. P. Shantarovich,[‡] K. Nagai,[§]
B. D. Freeman,[§] T. Masuda,[⊥] M. Teraguchi,[⊥] and G. Kwak[⊥]

A.V. Topchiev Institute of Petrochemical Synthesis, Russian Academy of Sciences, 29, Leninsky Pr., 119991, Moscow, Russia; N.N. Semenov Institute of Chemical Physics, Russian Academy of Sciences, 4, Kosygina Ul., 117977, Moscow, Russia; Chemical Engineering Department, North Carolina State University, Raleigh, North Carolina 27695-7905; and Department of Polymer Chemistry, Graduate School of Engineering, Kyoto University, 606-01 Kyoto, Japan

Received April 10, 2000; Revised Manuscript Received November 28, 2000

ABSTRACT: Gas permeation, sorption, and structural properties of two highly branched polyacetylenes, poly[1-phenyl-2-[*p*-(triphenylsilyl)phenyl]acetylene] (PPhSiDPA) and poly[1-phenyl-2-[*p*-(triisopropylsilyl)phenyl]acetylene] (PPrSiDPA), are reported. Structurally, both polymers have much in common; however, their transport properties are quite different. PPhSiDPA has dramatically lower permeability coefficients than PPrSiDPA. For example, the O₂ permeability coefficients of PPhSiDPA and PPrSiDPA are 12×10^{-10} and 230×10^{-10} cm³ (STP) cm/(cm² s cmHg), respectively, at 22 °C. Gas solubility is very high in PPrSiDPA, similar to that observed in poly(1-trimethylsilyl-1-propyne) (PTMSP), the most permeable polymer known. Gas solubility coefficients of PPhSiDPA are 2–3 times lower than those of PPrSiDPA. Free volume size and size distribution were characterized using positron annihilation lifetime (PAL) spectroscopy. Results from these studies (i.e., a bimodal size distribution of free volume elements and large free volume element size) are consistent with the observed transport and sorption properties of PPrSiDPA. In contrast, the PAL spectrum of PPhSiDPA is similar to that of conventional low free volume glassy polymers.

Introduction

Since the discovery of poly(1-trimethylsilyl-1-propyne) (PTMSP),¹ the gas permeation properties of substituted polyacetylenes have attracted much attention. So far, gas permeability, diffusivity, and, to a lesser extent, solubility values have been reported for approximately 30 amorphous polyacetylenes, whose generic chemical structure is given by $-\text{CR}=\text{CR}'-$, where R and R' are alkyl, aryl, fluorine-, silicon-, and germanium-containing radicals.^{2–4} PTMSP is still the most permeable polymer known; for example, its oxygen permeability has been reported to be approximately 10 000 barrers (1 barrer = 10^{-10} cm³ (STP) cm/(cm² s cmHg)).⁵ PTMSP has many interesting and, in some cases, very unusual properties for a glassy polymer. For example, it exhibits (1) extremely large gas diffusion and solubility coefficients;^{2,6–10} (2) very inefficient chain packing based on wide-angle X-ray diffraction (WAXD) spectroscopy;¹¹ (3) the lowest density of all known polymers (which results in extremely large fractional free volume estimated from group contribution methods)^{6,8–10} and very high free volume as determined by positron annihilation methods;^{6,11–14} (4) higher permeability coefficients to large, condensable organic vapors (e.g., *n*-butane) than to even the smallest, weakly sorbed penetrants such as H₂ and He;^{9,10,15} (5) negative activation energies of permeation for both light gases (e.g., H₂, N₂, and O₂) and condensable hydrocarbons;^{2,16} (6) a strong suppres-

sion of light gas permeability (e.g., H₂) in the presence of more strongly sorbed components (e.g., C₃H₈);^{17,18} (7) a very weak ability to sieve penetrant molecules based on size despite a very high glass transition temperature (presumably above 250 °C)^{9,10} (typically, weakly size-sieving behavior is characteristic of rubbery polymers¹⁹); and (8) rapid physical aging at ambient temperature, resulting in unusually strong reductions in free volume (i.e., increases in density) and gas permeability relative to other glassy polymers.^{7,13,20–24}

These unusual properties derive from the primary and higher-order molecular structure of the polymer. PTMSP has low cohesive energy density, which contributes to the tendency for these stiff polymer chains to pack inefficiently. The very stiff nature of the polymer chains in PTMSP may also frustrate conformational rearrangement in the solid state to more efficiently packed structures.⁴ However, other molecular structural features (e.g., cis/trans ratio) also contribute significantly to the shape of PTMSP polymer chains and, presumably, to their solid-state packing properties and transport properties. In this regard, the cis/trans ratio has been shown to strongly influence the sorption and transport properties of polyacetylenes and other classes of polymers containing main-chain double bonds.^{25,26}

Interestingly, many polyacetylenes, even those with rather bulky side groups, can exhibit relatively low gas permeabilities.² For example, if two of the three methyl groups on the trimethylsilyl group of PTMSP are replaced with ethyl units, the oxygen permeability at 25 °C decreases to only 440 barrers. If one of the methyls on the trimethylsilyl group of PTMSP is replaced by a phenyl ring, the O₂ permeability at 25 °C is only 4.4 barrers, more than 3 orders of magnitude lower than that of PTMSP.²⁷ Therefore, this polymer family exhibits a strikingly wide range of gas permeabilities, prob-

[†] A.V. Topchiev Institute of Petrochemical Synthesis, Russian Academy of Sciences.

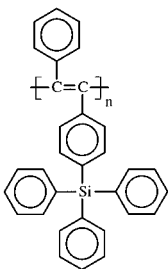
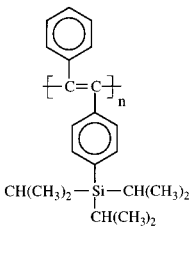
[‡] N.N. Semenov Institute of Chemical Physics, Russian Academy of Sciences.

[§] North Carolina State University.

[⊥] Kyoto University.

* Corresponding author: tel 011.7.095.955.4210, e-mail yampol@ips.ac.ru.

Table 1. Properties of Polyacetylenes

			
Acronym		PPhSiDPA	PPrSiDPA
M_w/M_n		2.7	2.5
Molecular mass, M_w		1.2×10^6	3.7×10^6
Onset of weight loss, $^{\circ}\text{C}$		430	270
Glass transition, $^{\circ}\text{C}$		> 430	> 270
Density, g/cm^3	geometric	1.16	1.00
	pycnometric	1.121	1.038
Fractional free volume ^a , %	geometric	13.0	15.0
	pycnometric	15.0	12.0

^a Based on the Bondi group contribution method.³¹

ably wider than that of any known class of organic polymers. As suggested elsewhere,²⁸ polyacetylenes exhibiting high gas permeability usually contain highly branched, nonpolar, symmetrically substituted, bulky side groups (e.g., $\text{Si}(\text{CH}_3)_3$ or $\text{Ge}(\text{CH}_3)_3$) attached directly (i.e., with no spacer) to the main chain. However, in general, structure/property paradigms for this family of polymers are not well-understood, and consequently, it is of interest to explore gas permeability and related physicochemical properties of other highly substituted polyacetylenes.

In this study, we report gas permeability, solubility, and diffusivity data for two silyl-substituted polyacetylenes: poly[1-phenyl-2-[*p*-(triphenylsilyl)phenyl]acetylene] (PPhSiDPA) and poly[1-phenyl-2-[*p*-(triisopropylsilyl)phenyl]acetylene] (PPrSiDPA). In addition, the free volume distribution was characterized using positron annihilation lifetime (PAL) spectroscopy.

Experimental Section

Polymerization. Monomers were synthesized from 1-(*p*-bromophenyl)-2-phenylacetylene and the corresponding trisubstituted chlorosilane as described by Teraguchi and Masuda.²⁹ Polyacetylenes were prepared using TaCl_5 as the catalyst and $n\text{-Bu}_4\text{Sn}$ as the cocatalyst. The catalyst, cocatalyst, and monomer concentrations were 20, 40, and 100 mM, respectively. Polymerizations were performed in toluene at $80\text{ }^{\circ}\text{C}$, and the reaction time was 24 h. ^1H and ^{13}C NMR and FT-IR analyses of the polymers confirmed the chemical structures in Table 1. The polymers are not soluble in hydrogen-bonding solvents such as methanol. However, they are soluble in toluene and chloroform. Both polymers formed strongly colored yellow or red-orange films depending on the thickness.

Film Preparation. Isotropic, dense films were prepared by casting from toluene solution (1–2 wt %) onto a glass plate. The plate was covered with a glass dish to slow the rate of solvent evaporation. Films were dried at ambient conditions for 2–4 weeks depending on film thickness and subsequently exposed to vacuum for up to 48 h to remove residual solvent. Some as-cast films were used directly for gas permeation and sorption experiments. Other as-cast films (10–40 μm in thickness) were stored (i.e., aged) at ambient conditions before testing. Films were not presoaked in a conditioning agent, such as methanol, prior to study.

Characterization. Two methods were used to determine film densities at ambient conditions. The geometric density was determined from the ratio of film weight to film volume. The pycnometric density is based on the difference of a sample's weight in air and in a nonsolvent (2-propanol in our study) of known density.³⁰ The results of both methods coincided within the measurement uncertainty ($\pm 0.06\text{ g}/\text{cm}^3$). Fractional free volume (FFV) was estimated according to Bondi's method:

$$\text{FFV} = (V_{\text{sp}} - 1.3 V_{\text{w}})/V_{\text{sp}} \quad (1)$$

where $V_{\text{sp}} = 1/\rho$ is the polymer specific volume, ρ is polymer density, and V_{w} is the estimated van der Waals volume of the repeat unit, calculated using a group contribution method.³¹ Wide-angle X-ray diffraction spectra (filtered Cu K α radiation) were obtained using a generator with rotating anode "RIGAKU" X-ray diffractometer (12 kW).

PAL spectra were recorded at room temperature in an inert atmosphere (N_2) with an Ortec "fast-fast" lifetime spectrometer. The time resolution was 230 ps (fwhm). We used a nickel-foil-supported [^{22}Na] sodium chloride radioactive positron source. Contributions from annihilation in the source and instrumental resolution were considered in the PATFIT and CONTIN data analysis programs. The integral statistics for each spectrum were $(1.5\text{--}2.0) \times 10^7$ coincidences. Each final PAL spectrum was obtained by summing the results of many cycles of measurements (10^6 counts per cycle). The CONTIN spectral analysis program determined a solution corresponding to a regularization parameter value, α , of $\sim 10^{-4}$, which represents the solution having a Fisher F -probability closest to 0.5. Application of the PATFIT program to each cycle gave satisfactory values of the variance of the fit ($\varphi \approx 1.05$) if the number of components (three or four) was determined correctly. To perform measurements in inert (nitrogen) atmosphere, the samples were placed in a rubber bag, which was then filled with dry nitrogen.

Gas Permeation. Two methods were used to characterize the permeability of these polyacetylenes to the following gases: He , H_2 , N_2 , O_2 , CH_4 , C_2H_6 , C_3H_8 , $n\text{-C}_4\text{H}_{10}$, and CO_2 . A mass spectrometer-based method³² was used to determine pure-gas, low-pressure permeability coefficients, P , of PPrSiDPA and PPhSiDPA samples at $22 \pm 2\text{ }^{\circ}\text{C}$. The upstream pressure was 50–500 mmHg, and the downstream pressure was about 10^{-3} mmHg. Diffusion coefficients, D , were estimated by the time-lag method, and solubility coefficients, S , were estimated from the ratio of permeability to diffusivity.

Pure-gas permeabilities of PPrSiDPA films were also characterized using a higher pressure, constant-pressure/variable-volume method at $35\text{ }^{\circ}\text{C}$.^{33,34} The feed pressure was 4.4 atm for all gases except n -butane (1.7 atm); the permeate pressure was maintained at 1 atm. Thus, both feed and permeate pressures were higher than for the mass spectrometer-based technique.

Gas Sorption. Propane and n -butane sorption isotherms in PPrSiDPA films were determined at $35\text{ }^{\circ}\text{C}$ using a Cahn 2000 electrobalance sorption system.³⁴ After loading the polymer film into the sample chamber, the sorption system was evacuated for 20–24 h at $35\text{ }^{\circ}\text{C}$ to degas the polymer film. Hydrocarbon penetrant was then introduced into the sorption chamber, and penetrant uptake was recorded as a function of time.

Results and Discussion

Characterization. On the basis of wide-angle X-ray diffraction results, both polyacetylenes are wholly amorphous. The WAXD spectrum of each polymer consists of three broad peaks. For PPrSiDPA, the more intense peaks have maxima at approximately 5° (2θ) and 15° , and there is a very weak peak in the range of 20° – 30° . For PPhSiDPA, the peak maxima are located at 5° , 13° , and 18° (2θ). A qualitative comparison suggests that the fraction of more densely packed chains (i.e., those

Table 2. Transport Parameters of PPhSiDPA at 22 °C Determined Using Mass Spectrometer-Based Permeation Apparatus

gas	P^a	$D \times 10^7{}^b$	S^c
H ₂	51.7		
He	33.0		
O ₂	12.1	1.22	0.75
N ₂	2.78	0.515	0.41
CO ₂	78.8	0.91	6.6
CH ₄	5.58	0.238	1.8
C ₂ H ₆	3.25	0.042	5.9

^a P in barrers, where 1 barrer = 10^{-10} cm³ (STP) cm/(cm² s cmHg). ^b D in cm²/s. ^c S in cm³ (STP)/(cm³ atm).

associated with the small interchain distance or, equivalently, highest 2θ value) is larger in PPhSiDPA than in PPrSiDPA.

Although the repeat units of these polyacetylenes have much in common with that of PTMSP, their densities and estimated fractional free volumes are quite different from that of PTMSP. Geometric and pycnometric densities of PPhSiDPA are 1.16 ± 0.04 and 1.121 ± 0.005 g/cm³, respectively. PPrSiDPA is less dense; it has geometric and pycnometric densities of 1.00 ± 0.06 and 1.038 ± 0.005 g/cm³, respectively. These values are much larger than those reported for PTMSP, which has density values as low as 0.6–0.7 g/cm³.^{3,6,8,11,35–37} Based on the data in Table 1, the FFV values of PPrSiDPA and PPhSiDPA are much lower than that of PTMSP (0.29–0.32) and similar to those of conventional glassy polymers, such as polycarbonates or polysulfones (cf. Paul and Yampolskii,²⁸ p 102).

Transport Properties of PPhSiDPA. The permeability, diffusivity, and solubility of PPhSiDPA determined using the low-pressure mass spectrometer-based technique are presented in Table 2. A comparison with other polyacetylenes containing phenyl groups² or polystyrenes³⁸ indicates that PPhSiDPA exhibits rather low gas permeability coefficients even though it contains bulky phenyl groups symmetrically substituted on the Si atom. The low permeability may be related to the ability of flat phenyl groups to stack, thereby forming more densely packed matrices than observed in other polyacetylenes bearing symmetrical, highly branched substituents. This rationale is consistent with the relatively high density, low free volume, and PAL results (discussed later). The tendency of glassy polymers containing aromatic rings to undergo short-range stacking of the phenyl rings parallel to one another in amorphous regions has been reported for poly(ethylene terephthalate).³⁹ In addition, π - π interactions and inductive effects favor electron shift from phenyl rings toward the Si atom,⁴⁰ possibly causing dipole-dipole interactions between chains which should promote efficient chain packing and, hence, lower permeability and diffusivity.

Masuda et al.² report properties of a wide range of substituted acetylene polymers, including several poly-(1-phenyl-2-alkylacetylenes). Based on these studies, large changes in the alkyl side group structure hardly influences gas permeation parameters. For example, oxygen permeability values range from 6 to 14 barrers as the pendent alkyl group size increases from methyl to *n*-hexyl. The oxygen permeability of PPhSiDPA is in this same range. Therefore, highly branched substituents based primarily on phenyl rings results in relatively densely packed polymers. No time dependence of permeability (i.e., physical aging) was observed for this

Table 3. Selectivity of Substituted Polyacetylenes

gas pair	PPhSiDPA	PPrSiDPA	PTMSP ^a
O ₂ /N ₂	4.4	2.5	1.4
H ₂ /N ₂	18.6	5.8	2.3
H ₂ /CH ₄	9.3	2.2	1.0
CO ₂ /CH ₄	14.1	5.4	1.8
CO ₂ /N ₂	28.3	14.2	4.1

^a Pure gas selectivity values for PTMSP were calculated based on permeability coefficients from Merkel et al.⁹ evaluated at $\Delta p = 0$ and 35 °C.

polymer based on repeated permeability measurements during 1 month.

Ideal separation factors, α_{ij} (which is equal to P_i/P_j , where P_i and P_j are pure gas permeability coefficients), for PPhSiDPA are recorded in Table 3. Based on the permeability/selectivity tradeoff relations for these gas pairs,⁴¹ the data points for PPhSiDPA are near the middle of the data range for conventional glassy polymers.

Transport and Sorption Properties of PPrSiDPA. Entirely different results were obtained for the polyacetylene containing symmetrically substituted side groups with bulky isopropyl radicals. Teraguchi and Masuda reported O₂ permeability coefficients in the range 20–40 barrers,²⁹ whereas the present study revealed much larger O₂ permeability coefficients, in the range 130–230 barrers (depending upon measurement conditions). This large difference in permeability coefficients could be related to physical aging-induced reductions in permeability of the films studied by Teraguchi and Masuda.²⁹ Furthermore, PTMSP permeability increases with increasing film thickness,^{20–24} and some of the difference might be due to differences in film thicknesses of the samples characterized by Teraguchi and Masuda and those in this study. To determine whether these effects were important enough to cause the observed variation in reported permeability of this polymer, a detailed study of thickness and aging effects was undertaken in two regimes: (1) the infinite dilution regime (using the mass spectrometer-based permeation technique) and (2) at higher pressures using the constant pressure/variable volume method described earlier.

Based on results from both types of experiments, permeability increases with increasing thickness. For example, the permeability of PPrSiDPA to methane at 35 °C is 93 and 149 barrers in as-cast films of 20 and 41 μ m thickness, respectively.³⁴ In addition, films in the range 20–40 μ m thick are prone to rapid aging as indicated by a steady decrease in gas permeability over time.³⁴ On the other hand, films thicker than 70 μ m do not age noticeably over the course of several weeks. The thicker films are, therefore, more convenient for a detailed investigation of the effects of penetrant size and properties on transport parameters.

The permeability, diffusion, and solubility coefficients of PPrSiDPA are presented in Table 4. This table contains permeability coefficients determined by the two methods described earlier. Data for PTMSP are provided for comparison. The permeability coefficients of PPrSiDPA given in the first column were determined using the mass spectrometer method, where the upstream pressure is 50–500 mmHg, the downstream pressure is $\sim 10^{-3}$ mmHg, and the temperature is 22 °C. The film thickness is 144 μ m. The second column presents the permeability coefficients, which were determined at an upstream pressure of 4.4 atm (*n*-C₄H₁₀:

Table 4. Transport Parameters of As-Cast PPrSiDPA and PTMSP Films^a

gas	PPrSiDPA				PTMSP ^d		
	<i>P</i> ^b	<i>P</i> ^c	<i>D</i> × 10 ⁷	<i>S</i>	<i>P</i>	<i>D</i> × 10 ⁷	<i>S</i>
He	315	220					
H ₂	530	350			15 000	2600	0.44
O ₂	230	130	6.9	2.5	9 000	520	1.3
N ₂	91	58	5.1	1.4	6 600	440	1.1
CO ₂	1300	590	7.5	13	27 000	330	5.5
CH ₄	240	150	3.9	4.7	15 000	360	3.6
C ₂ H ₆	310	300	2.0	12	31 000	170	23
C ₃ H ₈	140	1200			38 000	140	71
<i>n</i> -C ₄ H ₁₀		5400			133 000		

^a The units of *P*, *D*, and *S* are the same as in Table 2. ^b These data were obtained using the mass spectrometer technique (upstream pressure = 50–500 mmHg, downstream pressure = ~10⁻³ mmHg, 144 μm thick film, 22 °C). ^c These data were obtained using the constant pressure, variable volume technique (upstream pressure = 4.4 atm (1.7 atm for *n*-C₄H₁₀), downstream pressure = 1 atm, 41 μm thick film, 35 °C). ^d Data from Merkel et al.⁹

1.7 atm) and a downstream pressure of 1 atm and 35 °C with a 41 μm thick film.³⁴ The sample used in these experiments was an as-cast film (i.e., it was not conditioned in methanol). It was prepared by solution casting followed by 3 weeks of drying at ambient conditions and, afterward, approximately 24 h under vacuum at ambient temperature to remove solvent.

Diffusion coefficients were determined from time lag measurements under the low-pressure conditions and 22 °C. Solubility coefficients were estimated as the ratio *P*/*D* (determined using the mass spectrometer method).

All PTMSP permeability, diffusivity, and solubility coefficients, except for that of *n*-butane, are taken from Merkel et al.⁹ and were determined at 35 °C. The permeability and diffusivity coefficients are extrapolated to zero transmembrane pressure difference, and the solubility coefficients are extrapolated to infinite dilution. Because the permeability and diffusivity are evaluated at zero transmembrane pressure difference rather than at infinite dilution, the product of solubility and diffusivity is not exactly equal to permeability for the more condensable gases, which exhibit significant curvature in the sorption isotherms at low pressure. The *n*-butane permeability coefficient is from Pinnau et al.¹⁸ and was determined at 25 °C, an upstream pressure of 2.2 atm, and a downstream pressure of 1 atm.

PPrSiDPA exhibits relatively large permeability coefficients. They are lower than those of PTMSP by only an order of magnitude and are comparable to those of poly(dimethylsiloxane) (PDMS), the most permeable rubbery polymer.⁴² Due to the traditional tradeoff between gas permeability and selectivity observed for weakly sorbing gases, PPrSiDPA is less selective than PPhSiDPA (cf. Table 3).

Another interesting feature of PPrSiDPA is the sequence of permeability coefficients of *n*-alkanes. For conventional glassy polymers, permeability decreases with increasing carbon number of *n*-alkanes due to the large decrease in diffusion coefficients with increasing molecular size in low free volume, highly size sieving glassy polymers.^{15,19} In contrast, some rubbery polymers, such as PDMS, exhibit increases in permeability as hydrocarbon size increases.⁴² In such weakly size-sieving materials, the increase in solubility with increasing hydrocarbon size more than offsets the modest decrease in diffusivity, so larger, more soluble penetrants are more permeable than smaller, weaker

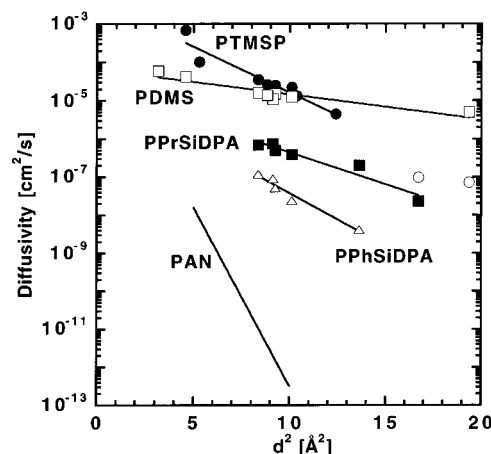


Figure 1. Correlation of diffusion coefficients with the square of effective penetrant cross-sectional diameter: PPrSiDPA, filled points 22 °C, open points 35 °C; PPhSiDPA, PDMS, PTMSP,⁴⁴ polyacrylonitrile, PAN.⁴⁵

sorbing penetrants. Many of the high free volume polyacetylenes, such as PTMSP and poly(4-methyl-2-pentyne) (PMP),³³ also exhibit this trend with increasing hydrocarbon size. These results are presumably due to large free volume levels in these polymers and an unusual distribution of free volume, which is discussed in more detail later.

The PPrSiDPA permeability coefficients determined in the low-pressure mass spectrometer-based experiments are somewhat different from those obtained with the high-pressure equipment. In particular, the former showed a maximum permeability value for propane, whereas the latter revealed a monotonic increase in permeability for the C₁–C₄ series of *n*-alkanes. The difference in the permeability coefficients of propane in the two types of experiments is probably due to the increase in propane diffusion coefficient with increasing penetrant concentration in PPrSiDPA.³⁴ The high-pressure equipment maintains a significantly higher average penetrant concentration in the polymer than the mass spectrometer method, and the diffusion coefficients of hydrocarbons such as propane will be higher in samples with higher propane concentrations. Additionally, the experiments were conducted at different temperatures, and this difference will contribute to differences in permeability coefficients measured by the two methods.

To provide some perspective of the diffusion coefficient values and their variation with penetrant size, Figure 1 presents a correlation of diffusivity in PPrSiDPA, PPhSiDPA, and other selected polymers with the square of the penetrant diameter, *d*². The *d*² values are from Teplyakov and Meares.⁴³ Rubbery polymers such as poly(dimethylsiloxane), PDMS, and PTMSP have very high diffusion coefficients and low diffusivity selectivity. Conventional glassy polymers (e.g., polyacrylonitrile) have low diffusion coefficients and high diffusivity selectivity. The polyacetylenes considered here have diffusivity selectivities similar to those of PDMS and PTMSP, but the diffusion coefficients are 2–3 orders of magnitude smaller. Our positron annihilation study (described below) suggests that these interesting features are related to the size distribution of elementary free volume in these polymers.

Interestingly, very large solubility coefficients were observed for PPrSiDPA, of the same order of magnitude

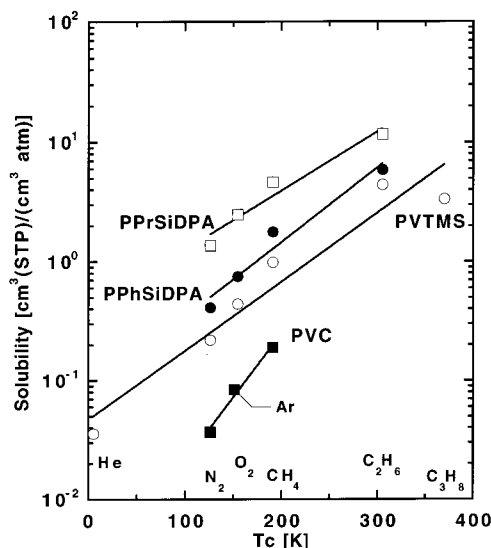


Figure 2. Correlation of solubility coefficients with penetrant critical temperature in PVTMS,⁴⁵ poly(vinyl chloride) [PVC],⁴⁶ PPrSiDPA, and PPhSiDPA.

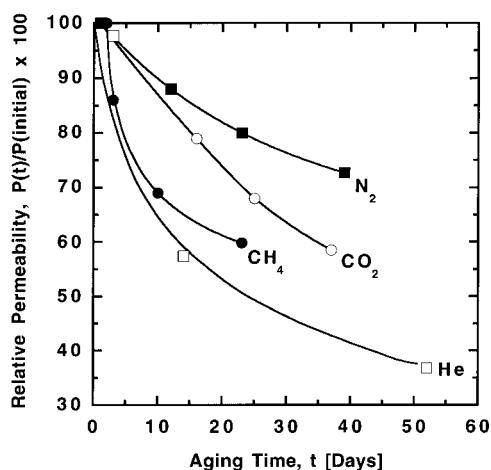


Figure 3. Aging of PPrSiDPA gas permeability in a vacuum at ambient temperature. The permeability coefficients were measured using the mass spectrometer method, and the film thickness was 37 μm . The initial permeability data were taken after 1 day for He, CO₂, and N₂ and after 2 days for CH₄.

as those of PTMSP. A comparison of the gas solubility coefficients of PPrSiDPA with those of PTMSP and other polymers is shown in Table 4. Figure 2 also presents a selection of these data. For some of the light gases, PPrSiDPA solubility coefficients are similar to or slightly larger than those in PTMSP. However, it is not clear that penetrant solubility is uniformly higher in PPrSiDPA than in PTMSP. The sample preparation history for the PPrSiDPA and PTMSP samples are somewhat different, and this may contribute to some of the differences in solubility between the two polymers. However, the difference in solubility among these two polymers is not sufficient to explain the differences in permeability, so the permeability differences between PPrSiDPA and PTMSP are due primarily to differences in diffusion coefficients, with PTMSP having much higher diffusion coefficients than PPrSiDPA.

Aging of PPrSiDPA. Like PTMSP, the permeability coefficients of PPrSiDPA decrease over time. This behavior is presented in Figure 3 for several gases. These results were obtained for a film stored in a vacuum-tight permeation cell with only brief exposure

Table 5. Effects of Aging on Gas Permeation Properties of PPrSiDPA^a

gas	permeability ³⁴ [barrers]		gas	permeability ³⁴ [barrers]	
	as-cast	aged		as-cast	aged
H ₂	260	100	CH ₄	93	38
O ₂	100	39	C ₃ H ₈	880	330
N ₂	44	18	<i>n</i> -C ₄ H ₁₀	4600	1800
CO ₂	560	240			

^a The samples were 20 μm thick. The aging protocol was storage for 7 days at ambient conditions following drying.

Table 6. Effect of Aging on Infinite Dilution Hydrocarbon Solubility in As-Cast and Aged PPrSiDPA Films³⁴

gas	<i>S</i> , cm ³ (STP)/(cm ³ atm)	
	as-cast ^a	aged ^b
C ₃ H ₈	70	31.9
<i>n</i> -C ₄ H ₁₀	330	216

^a The thickness of as-cast film samples was approximately 70 μm . After casting from solution, these films were dried at ambient conditions for 3 weeks and then placed in a vacuum oven for approximately 24 h to remove residual solvent. Sorption studies were undertaken immediately after the vacuum oven solvent removal step. ^b The thickness of aged film samples was 20 μm . After casting from solution, these films were dried at ambient conditions for 2 weeks and then placed in a vacuum oven for approximately 24 h to remove residual solvent. After the vacuum oven solvent removal step, these films were stored at ambient conditions for 3 weeks before beginning sorption studies.

to vacuum generated by an oil-containing vacuum pump before each measurement. The rate of gas permeability reduction is a strong function of film thickness. A very thick, 144 μm film exhibited no measurable changes in permeability over a 2 week time period. This behavior is consistent with that reported for PTMSP. Permeability of thin PTMSP films (40 μm) decreased by an order of magnitude during several hours whereas permeability of a thick film (ca. 100 μm) decreased by only 30% during 2 months.²³

Qualitatively, the aging results obtained using the mass spectrometer permeability method were also verified using the constant volume/variable pressure method. Table 5 shows that permeability coefficients of a 20 μm film decrease by a factor of 2–2.5 during 1 week of storage in ambient conditions. Permeability coefficients presented in this table were determined at an upstream pressure of 4.4 atm (*n*-C₄H₁₀: 1.7 atm) and a downstream pressure of 1 atm. The temperature was 35 °C. As-cast films were prepared by solution casting followed by 2 weeks of drying at ambient conditions and, afterward, approximately 24 h under vacuum at ambient temperature to remove solvent. The aged film was prepared by allowing an as-cast sample to age at ambient conditions for 7 days following the vacuum treatment for solvent removal. The initial (i.e., as-cast) permeability coefficients reported in Table 5 are somewhat lower than those reported in Table 4, probably due to differences in sample thickness. Table 5 reports data for a thinner sample, which ages more rapidly than thicker samples, and this thinner sample exhibits lower permeability under the same preparation and measurement conditions than its thicker analogue, whose data are reported in Table 4.

Aging of PPrSiDPA is also manifested in sorption properties of thin films of this polymer. For example, Table 6 presents infinite dilution solubility coefficients of propane and *n*-butane in PPrSiDPA. It is obvious that

the solubility coefficients are markedly reduced after aging.

Recently, McCaig and Paul observed aging as revealed by reduction in permeability of an entirely different type of polymer—a polyarylate made from bisphenol A benzophenone dicarboxylic acid.⁴⁷ Their studies also show that permeability decreases significantly faster in thin films (0.25 μm) than in thick films (33 μm). They attribute such thickness-dependent physical aging to the diffusion of free volume elements or holes to the film surface, where they are eliminated.⁴⁷ This mechanism may be important in describing the influence of thickness and aging on the permeation properties of PPrSiDPA.

Positron Annihilation Study. Positron annihilation lifetime (PAL) spectroscopy is a method employing positrons (e^+) as probes of free volume in polymeric materials. When positrons enter a material, they can exist, until their annihilation, as free positrons or in a bound state, namely the hydrogen-like positronium (Ps) particle (e^+e^-). Orthopositronium (o-Ps) particles localize in free volume elements (FVEs) within a polymer matrix, and their lifetime is interpreted as a measure of characteristic size of the free volume elements.⁴⁸

In conventional low free volume polymers, the PAL spectrum, which represents the distribution of time intervals between positron generation and annihilation, is interpreted as a sum of three exponential terms. This is an example of the finite term analysis approach, and the experimental data are often analyzed using a computer program such as PATFIT.⁴⁹ Only the third term, which corresponds to the longest lifetime, yields information about the size and concentration of FVEs. Usually this lifetime, τ_3 , is in the range 2–3 ns. Larger FVEs, which have lower average electron density than the surrounding polymer matrix, have longer o-Ps lifetimes. A relationship between FVE size and observed o-Ps lifetime has been formulated.^{50,51} This connection is expressed in the following semiempirical relation between the o-Ps lifetime, τ_3 (ns), and the mean radius, R (Å), of FVEs:⁵²

$$\tau_3 = 0.5\{1 - (R/R_0) + \frac{1}{2}\pi[\sin 2\pi(R/R_0)]\} \quad (2)$$

where $R_0 = R + \Delta R$ and ΔR , an empirical parameter characterizing the thickness of the electron layer in the FVE, is usually set to 1.66 Å. Different approaches have been suggested to calculate the concentration of FVEs in a polymer matrix and, in turn, the fractional free volume based on PAL spectra.^{53–55} In addition to the finite-term analysis approach, PAL spectra in polymers can also be interpreted using a continuous distribution of lifetimes and, therefore, a continuous FVE size distribution.^{56–58} A computer program such as CONTIN is used for this analysis.

The lifetime spectra of high permeability polymers like PTMSP and amorphous fluoropolymers based on 2,2-bis(trifluoromethyl)-4,5-difluoro-1,3-dioxole and tetrafluoroethylene (so-called Teflon AF) cannot be approximated by three component distributions.^{12,59} A fourth component, with a much longer lifetime than is observed in conventional polymers, is necessary to obtain a good fit of the model to the experimental data. Table 7 presents results of a finite term analysis of the PAL spectra for acetylene polymers studied in the present work. Only those components (i.e., the third and fourth components) of the spectra related to o-Ps an-

Table 7. Positron Annihilation Lifetime Spectra in N_2 Atmosphere

polymer	τ_3 , ns	τ_4 , ns	I_3 , %	I_4 , %
PPhSiDPA	2.01 ± 0.08	3.12 ± 0.01	21.13 ± 2.20	15.60 ± 2.47
PPrSiDPA	3.30 ± 0.07	9.38 ± 0.10	16.45 ± 0.40	28.16 ± 0.46
PTMSP	2.68 ± 0.45	10.9 ± 0.22	4.37 ± 0.48	33.80 ± 0.63

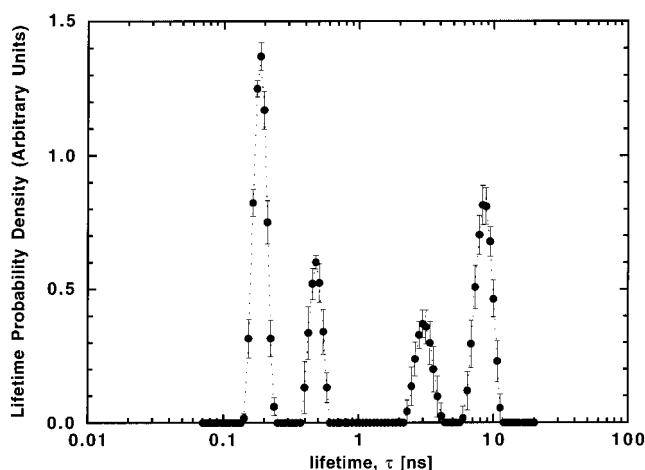


Figure 4. PAL spectrum obtained by CONTIN data analysis of PPrSiDPA.

nihilation in FVEs are presented. The spectra of both PPrSiDPA and PTMSP require four lifetime components to adequately describe the experimental data. The τ_4 values in these two polymers are much longer than o-Ps lifetimes in conventional glassy polymers such as polycarbonate and polystyrene.⁶⁰ Thus, the sizes of FVEs in these polymers should be significantly larger than in common polymers. Interestingly, o-Ps lifetimes and, therefore, FVE distributions of PPrSiDPA are, like PTMSP,^{12,13} bimodal. On this basis, the FVE structure of PPrSiDPA may be rather similar to that in PTMSP, which has been interpreted as a densified polymer matrix containing rather large free volume elements (with an average radius of 7.5 Å) connected by channel-like free volume elements with a smaller average radius.

An analysis of the experimental data based on the CONTIN approach leads to conclusions for PPrSiDPA that are consistent with that obtained using the finite-term analysis approach (PATFIT). Figure 4 presents the four component lifetime distribution obtained from a CONTIN analysis of the PPrSiDPA data. The two lifetime components below 1 ns are not related to o-Ps annihilations in the free volume of the polymer, and they will not be discussed further. The spectrum clearly shows two lifetime components at lifetimes substantially greater than 1 ns, and these are associated with o-Ps annihilations in the polymer FVEs. A similar CONTIN lifetime distribution has been reported for PTMSP.⁴⁷ The coordinates of the maxima of the two longer lifetime components in the CONTIN description are in good agreement with the τ_3 and τ_4 values found using the PATFIT program.

Different results were obtained for PPhSiDPA. First, a PATFIT treatment of the positron annihilation decay curve assuming four components for the PAL spectrum gave rather similar values of τ_3 and τ_4 , 2.01 and 3.12 ns, respectively. Because of the similarity in the lifetimes, the CONTIN analysis of PPhSiDPA could not discern two separate peaks in the lifetime distribution function. The lifetimes in PPhSiDPA are similar to those in conventional polymers. Additionally, in the finite

Table 8. Radii and Volumes of Free Volume Elements from PATFIT Analysis of Positron Annihilation Lifetime Spectroscopy Results

polymer	R_3 , Å	R_4 , Å	V_3 , Å ³	V_4 , Å ³
PPhSiDPA	2.9	3.7	98	215
PPrSiDPA	3.8	6.4	235	1087
PTMSP	3.4	6.8	166	1323

Table 9. Concentration of Free Volume Elements and Fractional Free Volume Estimated from Positron Annihilation Lifetime Spectroscopy

free vol parameters	PPhSiDPA	PPrSiDPA	PTMSP
concn of smaller free vol elements, $N_3 \times 10^{-19} \text{ cm}^{-3}$	7.8	4.7	1.4
concn of larger free vol elements, $N_4 \times 10^{-19} \text{ cm}^{-3}$	3.5	4.9	6.1
free vol of larger free vol elements, (FFV) ₄ , %	0.80	5.4	8.1
total free vol (FFV) _p , %	1.6	6.4	8.3
amount of free vol in larger free vol elements (FFV) ₄ /(FFV) _p × 100 (%)	50	84	98

term analysis method, the PAL spectrum was described almost as well by a three-component model as by a four-component model. Therefore, the behavior of this polyacetylene is rather typical of that observed for conventional glassy polymers such as polycarbonate or polystyrene. Interestingly, different silyl group substituents (isopropyl vs phenyl) of otherwise structurally similar polyacetylenes apparently exert dramatic effects on free volume as probed by PAL spectroscopy.

Equation 2 permits an estimation of the radii of smaller (R_3) and larger (R_4) free volume elements in the polymers based on the τ_3 and τ_4 values, respectively. The results of these calculations are presented in Table 8 together with the corresponding average volumes of smaller and larger free volume elements in three polyacetylenes. These volume were calculated assuming a spherical form of free volume elements, that is $V_i = 4\pi(R_i^3)/3$, $i = 3$ or 4 . The R_4 and V_4 values in PPrSiDPA and PTMSP are similar and much larger than those in PPhSiDPA. The size of the smaller free volume elements, as characterized by R_3 and V_3 , is also larger in PPrSiDPA and PTMSP than in PPhSiDPA.

To estimate fractional free volume from PAL data, concentrations of the larger and smaller free volume elements must be evaluated. Recently, a model of diffusion-controlled trapping and decay of o-Ps in polymers was proposed.⁵⁵ Based on the PATFIT results, this model was used to estimate the concentration of smaller (N_3) and larger (N_4) free volume elements. The results are summarized in Table 9. The total fractional free volume from PAL spectroscopy, (FFV)_p, can be estimated as follows:

$$(\text{FFV})_p = N_3(4\pi R_3^3/3) + N_4(4\pi R_4^3/3) \quad (3)$$

The values of (FFV)_p as well as the contribution from the larger microcavities (FFV)₄ are also presented in Table 9. The absolute values of (FFV)_p are in the range 1.6–8.3% in the polymers studied, which is consistent with expectations based on the results of mechanical or physicochemical studies of amorphous polymers.⁵² The contribution of the larger free volume elements, (FFV)₄, to the total, (FFV)_p, is much larger for PTMSP and PPrSiDPA than for PPhSiDPA. In fact, much of the difference in the (FFV)_p values among this family of

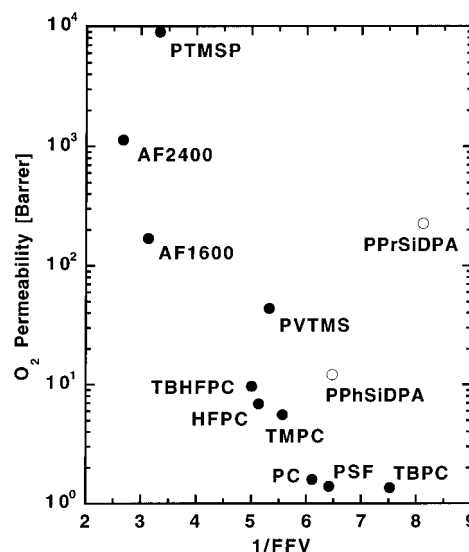


Figure 5. Correlation of oxygen permeability coefficients at 35 °C with fractional free volume as estimated by the Bondi group contribution method: PTMSP,⁹ Teflon AF2400 and AF1600,⁵⁹ PVTMS, tetrabromopolycarbonate (TBPC), tetrabromohexafluoropolycarbonate (TBHFPC), hexafluoropolycarbonate (HFPC), tetramethylpolycarbonate (TMPC), bisphenol A polycarbonate (PC), and polysulfone (PSF).²⁸

polymers is due to differences in the concentrations of the larger free volume elements.

Fractional free volume values based on density and group contribution methods, such as the Bondi method, (FFV)_B, and based on PAL spectroscopy are the most frequently cited in the literature. These approaches rely on different definitions and model assumptions. Therefore, in general, FFV values estimated by these methods do not coincide. However, they are often well correlated. For example, in a family of polycarbonates, (FFV)_B values are approximately twice as large as (FFV)_p values.⁶¹ In this work, both methods were used to characterize fractional free volume. For PPhSiDPA, PPrSiDPA, and PTMSP, (FFV)_B values are larger than (FFV)_p values by factors of approximately 9, 2, and 3, respectively.

Good correlations of (FFV)_B with D_i and P_i values in different polymers have been reported (see, e.g., ref 62). In this regard, polymers that exhibit extraordinarily large free volume element size based on PAL spectroscopy usually show very large Bondi fractional free volume values (e.g., PTMSP or Teflon AF^{12,59}). Interestingly, PPrSiDPA does not follow this trend; its low (FFV)_B values are in dramatic contrast to the large free volume element size indicated by PAL spectroscopy. Moreover, its (FFV)_B value is comparable to those of polymers having permeability coefficients orders of magnitude lower. In fact, similar values of (FFV)_B have been observed for poly(tetrabromopolycarbonate), whose O₂ permeability coefficient is 1.36 barrers (see Paul and Yampolskii,²⁸ p 102 and Table 4). Therefore, the permeation properties of PPrSiDPA are not well correlated with free volume based on the Bondi group contribution method. This point is illustrated in Figure 5, which presents a correlation of oxygen permeability with (FFV)_B for a variety of glassy polymers. The PPrSiDPA data point is not well described by the broad band of the correlation observed for the other polymers. These composite results suggest that either the group contribution parameters used in the Bondi method are not

appropriate for this polymer or the structure of the FVEs in PPrSiDPA is different from that of other glassy polymers. If the Bondi parameters are correct, the high permeability values may suggest a heterogeneous distribution of FVEs that favor high permeability. In this regard, the permeability of PPrSiDPA is much lower than that of PTMSP despite a similar size and concentration of FVE accessible to positrons, which suggests that the free volume elements in PTMSP are also organized in a fashion that is particularly suited to achieve high gas permeability coefficients.

Conclusions

The gas and vapor sorption, diffusion, and permeation properties of two structurally similar polyacetylenes, poly[1-phenyl-2-[*p*-(triphenylsilyl)phenyl]acetylene] (PPhSiDPA) and poly[1-phenyl-2-[*p*-(triisopropylsilyl)phenyl]acetylene] (PPrSiDPA), have been studied. Despite their structural similarities, these two polymers have very different transport parameters, solubility coefficients, tendency toward physical aging, free volume element size, and size distribution. The properties of PPhSiDPA suggest that it exhibits many permeability features similar to those of conventional glassy polymers. In contrast, PPrSiDPA is orders of magnitude more permeable than PPhSiDPA and exhibits properties similar to extremely high free volume glassy polymers such as PTMSP and PMP. Some of the interesting features of PPrSiDPA include (i) increasing gas permeability coefficients with increasing molecular size of *n*-alkanes, (ii) extraordinary large solubility coefficients of light gases, (iii) rapid physical aging manifested by reductions in gas permeability and solubility over time, (iv) rather large light gas permeability coefficients, in the range 10^2 – 10^3 barrers; and (v) large radii of free volume elements based on PAL spectroscopy (6.4 Å).

The fractional free volume of PPrSiDPA estimated from PAL results is in dramatic disagreement with that estimated using the Bondi group contribution method, which is based on polymer density. The free volume probed by PAL spectroscopy in PPrSiDPA is very high relative to conventional polymers, while the fractional free volume based on the Bondi method is similar to that of low permeability, conventional glassy polymers. If this observation is not related to an artifact in estimating free volume based on group contribution methods, then it suggests that the PPrSiDPA microstructure may include regions with large, possibly interconnected, free volume elements surrounded by rather densely packed regions. The superposition of these structures could be consistent with the observed rather high average density, low fractional free volume (based on density) and high permeability coefficients. The large free volume elements may account for high solubility coefficients and be the locus of rapid physical aging. The more densely packed regions could act as barriers to explain why permeability and diffusion coefficients of this polymer are significantly smaller than those of PTMSP despite similar values of free volume element sizes and total fractional free volume from PAL spectroscopy.

Acknowledgment. The research described in this publication was made possible in part by Award No. RC2-347 of the U.S. Civilian Research and Development Foundation for the Independent States of the Former Soviet Union (CRDF).

References and Notes

- (1) Masuda, T.; Isobe, E.; Higashimura, T.; Takada, K. *J. Am. Chem. Soc.* **1983**, *105*, 7473.
- (2) Masuda, T.; Iguchi, Y.; Tang, B.-Z.; Higashimura, T. *Polymer* **1988**, *29*, 2241.
- (3) Tsuchihara, K.; Masuda, T.; Higashimura, T. *Macromolecules* **1992**, *25*, 5816.
- (4) Savoca, A. C.; Surnamer, A. D.; Tien, C. *Macromolecules* **1993**, *26*, 6211.
- (5) Robeson, L. M.; Burgoyne, W. F.; Langsam, M.; Savoca, A. C.; Tien, C. F.; *Polymer* **1994**, *35*, 4970.
- (6) Plate, N. A.; Bokarev, A. K.; Kaliuzhnyi, N. E.; Litvinova, E. G.; Khotimskii, V. S.; Volkov, V. V.; Yampolskii, Yu. P. *J. Membr. Sci.* **1991**, *60*, 13.
- (7) Nakagawa, T. In *Polymeric Gas Separation Membranes*; Paul, D. R., Yampolskii, Yu. P., Eds.; CRC Press: Boca Raton, FL, 1994; p 399.
- (8) Ichiraku, Y.; Stern, S. A.; Nakagawa, T. *J. Membr. Sci.* **1987**, *34*, 5.
- (9) Merkel, T. C.; Bondar, V.; Nagai, K.; Freeman, B. D. *J. Polym. Sci., Part B: Polym. Phys. Ed.* **2000**, *38*, 273.
- (10) Morisato, A.; Shen, H.-C.; Sankar, S.; Freeman, B. D.; Casillas, C. G.; Pinnau, I. *J. Polym. Sci., Part B: Polym. Phys. Ed.* **1996**, *34*, 2209.
- (11) Yampolskii, Yu. P.; Shishatskii, S. M.; Shantarovich, V. P.; Antipov, E. M.; Kuzmin, N. N.; Rykov, S. V.; Khodjaeva, V. L.; Plate, N. A. *J. Appl. Polym. Sci.* **1993**, *48*, 1935.
- (12) Yampolskii, Yu. P.; Shantarovich, V. P.; Chernyakovskii, F. P.; Kornilov, A. I.; Plate, N. A. *J. Appl. Polym. Sci.* **1993**, *47*, 85.
- (13) Consolati, G.; Genco, I.; Pegoraro, M.; Zanderighi, L. *J. Polym. Sci., Part B: Polym. Phys.* **1996**, *43*, 357.
- (14) Shantarovich, V. P.; Azamatova, Z. K.; Novikov, Yu. A.; Yampolskii, Yu. P. *Macromolecules* **1998**, *31*, 3963.
- (15) Freeman, B. D.; Pinnau, I. *Trends Polym. Sci.* **1997**, *5*, 167.
- (16) Dixon-Garret, S. V.; Nagai, K.; Freeman, B. D. *J. Polym. Sci., Part B: Polym. Phys.* **2000**, *38*, 1078.
- (17) Srinivasan, R.; Auvil, S. R.; Burban, P. M. *J. Membr. Sci.* **1994**, *86*, 67.
- (18) Pinnau, I.; Casillas, C. G.; Morisato, A.; Freeman, B. D. *J. Polym. Sci., Part B: Polym. Phys. Ed.* **1996**, *34*, 2613.
- (19) Yampolskii, Yu. P.; Durgaryan, S. G.; Nametkin, N. S. *Vysokomol. Soed. B* **1979**, *21*, 616.
- (20) Nagai, K.; Freeman, B. D.; Hill, A. J. *J. Polym. Sci., Part B: Polym. Phys.* **2000**, *38*, 1222.
- (21) Tasaka, S.; Inagaki, N.; Igawa, M. *J. Polym. Sci., Part B: Polym. Phys.* **1991**, *29*, 691.
- (22) Shimomura, H.; Nakanishi, K.; Odani, H.; Kurata, M.; Masuda, T.; Higashimura, T. *Kobunshi Ronbunshu* **1986**, *43*, 747.
- (23) Asakawa, S.; Saitoh, Y.; Waragai, K.; Nakagawa, T. *Gas Sep. Purif.* **1989**, *3*, 117.
- (24) Langsam, M.; Robeson, L. M. *Polym. Eng. Sci.* **1989**, *29*, 44.
- (25) Morisato, A.; Miranda, N. R.; Freeman, B. D.; Hopfenberg, H. B.; Costa, G.; Grosso, A.; Russo, J. *J. Appl. Polym. Sci.* **1993**, *49*, 2065.
- (26) Yampolskii, Yu. P.; Finkelshtein, E. Sh.; Makovetskii, K. L.; Bondar, V. I.; Shantarovich, V. P. *J. Appl. Polym. Sci.* **1996**, *62*, 349.
- (27) Nagai, K.; Masuda, T.; Nakagawa, T.; Freeman, B. D.; Pinnau, I. *Adv. Polym. Sci.*, in press.
- (28) Paul, D. R.; Yampolskii, Yu. P., Eds.; *Polymeric Gas Separation Membranes*; CRC Press: Boca Raton, FL, 1994.
- (29) Teraguchi, M.; Masuda, T. *J. Polym. Sci., Part A: Polym. Chem.* **1998**, *36*, 2721.
- (30) Shishatskii, S. M. Thesis (kand. chem. sci), Moscow, TIPS, 1995.
- (31) Van Krevelen, D. W. *Properties of Polymers*; Elsevier: Amsterdam, 1990.
- (32) Yampolskii, Yu. P.; Novitskii, E. G.; Durgaryan, S. G. *Zavodsk. Lab.* **1980**, *46*, 256.
- (33) Morisato, A.; Pinnau, I. *J. Membr. Sci.* **1996**, *121*, 243.
- (34) Nagai, K.; Toy, L. G.; Freeman, B. D.; Teraguchi, M.; Masuda, T.; Pinnau, I. *J. Polym. Sci., Part B: Polym. Phys. Ed.* **2000**, *38*, 1474.
- (35) Witchev-Lakshmanan, L. C.; Hopfenberg, H. B.; Chern, R. T. *J. Membr. Sci.* **1990**, *48*, 321.
- (36) Jia, J.; Baker, G. L. *J. Polym. Sci., Part B: Polym. Phys.* **1998**, *36*, 959.
- (37) Nakanishi, K.; Odani, H.; Kurata, M.; Masuda, T.; Higashimura, T. *Polym. J.* **1987**, *19*, 293.

- (38) Puleo, A. C.; Muruganandam, N.; Paul, D. R. *J. Polym. Sci., Part B: Polym. Phys.* **1989**, *27*, 2385.
- (39) Murthy, N. S.; Correale, S. T.; Minor, H. *Macromolecules* **1991**, *24*, 1185.
- (40) Petrov, A. D.; Mironov, V. F.; Ponomarenko, V. A.; Chernyshev, E. A. *Synthesis of Organo-silicon Monomers*; Nauka Publ.: Moscow, 1961.
- (41) Robeson, L. M. *J. Membr. Sci.* **1991**, *62*, 165.
- (42) Robb, W. L. *Ann. N.Y. Acad. Sci.* **1968**, *146*, 119.
- (43) Teplyakov, V.; Meares, P. *Gas Sep. Purif.* **1990**, *4*, 66.
- (44) Nakagawa, T.; Saito, T.; Asakawa, S.; Saito, Y. *Gas Sep. Purif.* **1988**, *2*, 6.
- (45) Teplyakov, V. *Zh. Vses. Khim. Ob.* **1987**, *32*, 695.
- (46) Tikhomirov, B. P.; Hopfenberg, H. B.; Stannett, V. T.; Williams, J. L. *Macromol. Chem.* **1968**, *118*, 177.
- (47) McCaig, M. S.; Paul, D. R. *Polymer* **2000**, *41*, 629.
- (48) Shrader, D. M.; Jean, Y. C., Eds.; *Positron and Positron Chemistry*; Elsevier: Amsterdam, 1988.
- (49) PATFIT88: A data-processing system for PAL spectra on mainframe and PC. Kirkegard, P.; Pedersen, N. J.; Eldrup, M. Risoe National Laboratory, DK-4000, Roskilde, Denmark, Risoe-M-2740.
- (50) Tao, S. J. *J. Chem. Phys.* **1972**, *56*, 5499.
- (51) Eldrup, M.; Lightbody, D.; Sherwood, J. N. *Chem. Phys.* **1981**, *63*, 51.
- (52) Nakanishi, H.; Wang, S. J.; Jean, Y. C. In *Positron Annihilation Studies of Fluids*; Sharma, S. C., Ed.; World Science: Singapore, 1988; p 292.
- (53) Hristov, H. A.; Bolan, B.; Ye, A. F.; Xie, L.; Gidley, D. W. *Macromolecules* **1996**, *29*, 8507.
- (54) Dlubek, G.; Saarinen, K.; Fretwell, H. M. *J. Polym. Sci., Part B: Polym. Phys.* **1998**, *36*, 1513.
- (55) Shantarovich, V. P.; Goldanskii, V. I. *Hyperfine Interact.* **1998**, *116*, 67.
- (56) Provencher, S. W. *Comput. Phys. Commun.* **1982**, *27*, 229.
- (57) Gregory, R. B. *J. Appl. Phys.* **1991**, *70*, 4665.
- (58) Deng, Q.; Jean, Y. C. *Macromolecules* **1993**, *26*, 30.
- (59) Alentiev, A. Yu.; Yampolskii, Yu. P.; Shantarovich, V. P.; Nemser, S. M.; Plate, N. A. *J. Membr. Sci.* **1997**, *126*, 123.
- (60) Goldanskii, A. V.; Onishuk, V. A.; Shantarovich, V. P.; Volkov, V. V.; Yampolskii, Yu. *Khim. fiz.* **1988**, *7*, 616.
- (61) Jean, Y. C.; Yuan, J. P.; Liu, J.; Deng, Q.; Yang, H. *J. Polym. Sci., Part B: Polym. Phys.* **1995**, *33*, 2365.
- (62) Maeda, Y.; Paul, D. R. *J. Polym. Sci., Part B: Polym. Phys.* **1987**, *25*, 1005.

MA000628U